Nucleus

ISSN: 1949-1034 (Print) 1949-1042 (Online) Journal homepage: https://www.tandfonline.com/loi/kncl20

Differential staining of peripheral nuclear chromatin with Acridine orange implies an A-form epichromatin conformation of the DNA

Jekaterina Erenpreisa, Jekabs Krigerts, Kristine Salmina, Turs Selga, Hermanis Sorokins & Talivaldis Freivalds

To cite this article: Jekaterina Erenpreisa, Jekabs Krigerts, Kristine Salmina, Turs Selga, Hermanis Sorokins & Talivaldis Freivalds (2018) Differential staining of peripheral nuclear chromatin with Acridine orange implies an A-form epichromatin conformation of the DNA, Nucleus, 9:1, 171-181, DOI: 10.1080/19491034.2018.1431081

To link to this article: https://doi.org/10.1080/19491034.2018.1431081

NUCLEUS
2018, VOL. 9, NO. 1, 171–181
https://doi.org/10.1080/19491034.2018.1431081

Taylor & Francis
Taylor & Francis Group

ORIGINAL RESEARCH

OPEN ACCESS Check for updates

Differential staining of peripheral nuclear chromatin with Acridine orange implies an A-form epichromatin conformation of the DNA

Jekaterina Erenpreisa [a,+], Jekabs Krigerts[a,b], Kristine Salmina[a], Turs Selga[c], Hermanis Sorokins[b] and Talivaldis Freivalds[d,+]

[a]Latvian Biomedical Research & Study Centre, Ratsupites 1, Riga, Latvia; [b]Institute of Biomedical Engineering and Nanotechnologies, Riga Technical University, Kalku iela 1, Riga, Latvia; [c]Faculty of Biology, University of Latvia, Raina bulvaris 19, Riga, Latvia; [d]Institute of Kardiology and Regenerative Medicine, University of Latvia, Raina bulvaris 19, Riga, Latvia

ABSTRACT

The chromatin observed by conventional electron microscopy under the nuclear envelope constitutes a single layer of dense 30–35 nm granules, while ~30 nm fibrils laterally attached to them, form large patches of lamin-associated domains (LADs). This particular surface "epichromatin" can be discerned by specific (H2A+H2B+DNA) conformational antibody at the inner nuclear envelope and around mitotic chromosomes. In order to differentiate the DNA conformation of the peripheral chromatin we applied an Acridine orange (AO) DNA structural test involving RNAse treatment and the addition of AO after acid pre-treatment. MCF-7 cells treated in this way revealed yellow/red patches of LADs attached to a thin green nuclear rim and with mitotic chromosomes outlined in green, topologically corresponding to epichromatin epitope staining by immunofluorescence. Differentially from LADs, the epichromatin was unable to provide metachromatic staining by AO, unless thermally denatured at 94°C. DNA enrichment in GC stretches has been recently reported for immunoprecipitated ~ 1Kb epichromatin domains. Together these data suggest that certain epichromatin segments assume the relatively hydrophobic DNA A-conformation at the nuclear envelope and surface of mitotic chromosomes, preventing AO side dimerisation. We hypothesize that epichromatin domains form nucleosome superbeads. Hydrophobic interactions stack these superbeads and align them at the nuclear envelope, while repulsing the hydrophilic LADs. The hydrophobicity of epichromatin explains its location at the surface of mitotic chromosomes and its function in mediating chromosome attachment to the restituting nuclear envelope during telophase.

ARTICLE HISTORY
Received 25 September 2017
Revised 6 January 2018
Accepted 18 January 2018

KEYWORDS
acridine orange; DNA structural test; DNA A-form; epichromatin; nucleosome superbeads; LADs; NADs

Introduction

The last decade boosted interest in the nuclear periphery chromatin domains and their role in the nuclear architecture and function. Using transfection with a chimeric gene containing lamin B fused to DNA methylase, followed by analysis of the methylated DNA fragments, the two fractions of heterochromatic, lamin-associated domains (LAD)s, which are 0.1–10 Mbp long, enriched in AT, and comprise ~40% of nuclear DNA, were discerned – constitutive (cLADs) and facultative (fLADs); the latter change compaction and activity depending on tissue differentiation pattern and transcription activity [1–4]. LADs form ~ 0.3–0.6 μm domains of the peripheral heterochromatin separated by nuclear pores. However, one more minor fraction of the peripheral chromatin, which directly aligns to the inner nuclear envelope, can be morphologically discerned. On conventional TEM sections of various cells and species the existence at the inner nuclear membrane of the tightly apposed array of chromatin granules 30–35 nm in diameter appear denser than the ~30 nm chromatin fibrils laterally attached to them and form variably bulky patches of less condensed heterochromatin. This was noted by early electron microscopists and is shown in Fig. 1 [5]. Investigation of this chromatin fraction and derived nuclear envelope-limited sheets started from 60–s [6]. A group from Moscow University [7] reported on the isolation of this fraction using its

CONTACT Jekaterina Erenpreisa katrina@biomed.lu.lv
[+]senior authors
Supplemental data for this article can be accessed on the publisher's website.

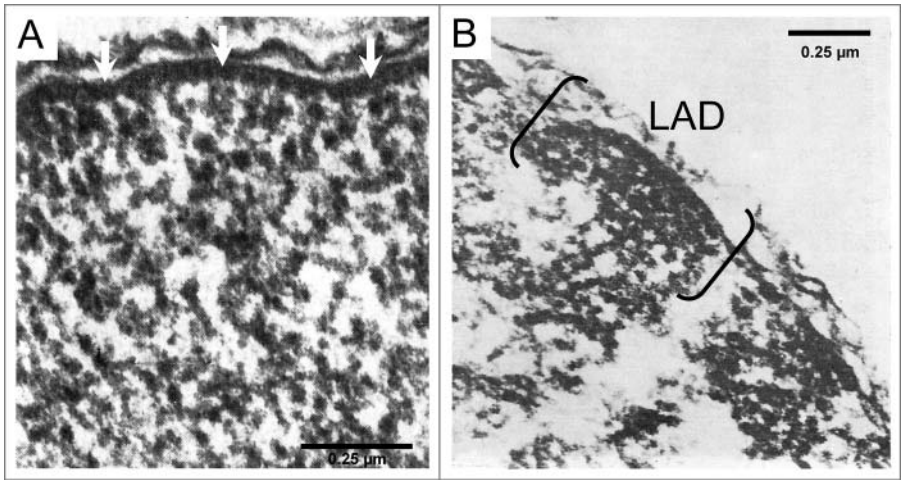

Figure 1. The particular chromatin fraction (presumed epichromatin) at the inner membrane of the nuclear envelope as revealed by transmission electron microscopy after conventional fixation and contrasting: (A) rat hepatocyte nucleus isolated on sucrose cushion. Epichromatin (arrows) forms a row of tightly arranged dense granules ~30 nm in diameter (arrows) set directly under the inner membrane of the nuclear envelope, while 27–30 nm thick, slightly coiled, chromatin fibrils appear laterally attached to it; (B) rat thymocyte nuclei, manually isolated by a homogeniser in isotonic solution, display the peripheral domains which form bulky condensed patches (presumed LADs) separated by nuclear pores and are tightly apposed to a more condensed layer of epichromatin under the nuclear envelope. Fig. 1 is republished from [5] with permission of the publisher.

DNAse resistance after cross-linking to the nuclear envelope with UV. They showed in rat liver that these dense chromatin granules bound to the nuclear envelope are forming a canonical nucleosome 'ladder". Donald and Ada Olins and colleagues found that this nuclear surface chromatin, coined by them "epichromatin", could be specifically detected by the monoclonal conformational antibody PL2-6 revealing a unique pattern of DNA interaction with nucleosomal histones H2A+H2B [8–10]. Epichromatin epitope is immuno-co-precipitated and roughly colocalised on confocal sections with the proteins of the inner nuclear envelope (lamin B receptor, LAP2β. SUN2, and anionic phophatidylserine) [9,11–13] granularly covering all the nuclear surface. However, epichromatin is also present at the surface of mitotic chromosomes in the absence of the nuclear envelope (NE), despite cytoplasmic dissipation of NE proteins [9]. Immunoelectron microscopy documented localization of the epichromatin epitope of PL2-6 antibody at the inner nuclear envelope [9] topologically corresponding to the chromatin layer of dense ~30 nm granules at the nuclear envelope seen in conventional electron microscopy.

The participation of epichromatin, and its derived nuclear envelope sheets, in providing anchorage of decondensing mitotic chromosomes to the restituting nuclear envelope in normal telophase, and in mitotic slippage, was evidenced by electron microscopy [8,14–16]. The latest papers from Olins, Teif and colleagues [13,17] revealed enrichment of epichromatin constituting 5% of the nuclear DNA with GC stretches, methylated CpGs, ALU transposons, poverty with AT stretches, preservation of the nucleosome repeats, and more dense nucleosome packaging than in general chromatin.

Still the conformation peculiarity of epichromatin and its relation to LADs remain poorly understood. In this paper we tried to address this issue by application of the acridine orange (AO) staining technique in the test sensitive to DNA conformation.

AO is a cationic aromatic compound capable of binding to both nucleic acids. It binds DNA in two ways. In a stable monomeric form AO intercalates its planar acridine ring between the lower and upper purine and pyramidine rings of ~ each third nucleotide base pair, while its dimethyl-aminogroup electrostatically clamps the negatively charged PO_2^- of every strand. AO can also aggregate on DNA by weaker side binding of almost every nucleotide PO_2^- allowing co-planar dye dimerisation [18,19]. By intercalation it produces a green emission peak of the monomeric dye form (max ~530 nm), while the AO dimers produce a red emission peak (max 640 nm). Both can be excited by an argon laser (488 nm) using a confocal microscope or I3 optical filter with a Leica epifluorescence microscope. Denaturation of DNA to single strands in water

solutions causes a sharp shift from green to red fluorescence [18]. However, on whole nuclei of fixed, *in situ* cells both forms of AO binding to the chromatin are usually present, albeit in different proportions. With the increase of DNA intercalation affinity for AO the electrostatic binding of the nucleosome histones to DNA neutralizing its negative charge, is also increased diminishing the chromatin capacity of AO side dimerisation [20,21]. Therefore, a short provocative acid pre-treatment, when applied after RNA extraction in the AO DNA structural test, allows the discrimination between these states competing for the dye binding and provides information both on the DNA secondary structure and the DNA packaging pattern in different chromatin categories (e.g. it is widely used for the differentiation between mature and immature sperm nuclei) [22–25]. Here this methodology, in the variant combined from the protocols of Roschlau [26] and Rigler [18,27] (using a relatively high AO concentration at a relatively low pH – as the most sensitive to DNA conformational states *in situ*) allowed us to reveal a peculiar DNA conformation of the epichromatin. This was different from the two other forms of peripheral chromatin corresponding LADs.

Results

Spectral characteristics of AO staining of cell nuclei

After application of the AO test by the protocol described in Methods, both monomeric (max emission 530 nm) and di-(poly)-meric (max emission 635–640 nm) spectral peaks are excited by an argon laser (488 nm) in whole cell nuclei, as measured using a confocal microscope (The underlying research materials can be accessed at Supplemental Fig. 1). Interphase cell nuclei are rather heterogeneous after AO staining (perhaps depending on their functional state) while mitotic chromosomes are more orange than interphase cell nuclei. Both interphase nuclei and mitotic chromosomes are outlined with a thin, AO-fluorescing green rim.

Preservation of the epichromatin epitope

When applying the combined immunofluorescent staining for lamin B1 and epichromatin by specific monoclonal antibodies, after fixation with ethanol/acetone and treatment with RNAse, as used in the AO test (but also adding post-fixation with fresh formaldehyde (PFA) as recommended by Olins et al. [9],) we found good preservation of lamin B, the epichromatin epitope, highlighted also around mitotic chromosomes, and well preserved nuclear DNA post-stained with DAPI (Supplemental Fig. 2 A-C). So, together with spectral studies, the applied AO protocol was judged adequate for our purpose to evaluate DNA conformation of the peripheral chromatin compartments including epichromatin.

AO tested conformation of the peripheral chromatin domains in interphase cells

Figure 2 presents the result of application, *in situ*, of the AO test to MCF-7 cells grown on chamberslides. In all experiments the cells were preliminary imaged using an epifluorescence microscope fitted with an AO in I3 Leica optical filter and then imaged using a confocal microscope with an argon laser within 2 hours after sealing under coverslips. The clear green outline is seen in interphase cell nuclei, which is different from the patched "sandwiches" of tightly apposed domains located inside, and stained yellow and orange/red (Fig. 2A). The topology of the green and orange/red components corresponds to the topology of the epichromatin and LAD domains seen by conventional electron microscopy (Fig. 1). This three-coloured compartmentalisation of the nuclear periphery is particularly well seen in very early prophase cells (Fig. 2B). The inner heterochromatin "sandwiches" become better differentiated from the green epichromatin after extending the provocative acid pretreatment from 40 sec to 5 min (Fig. 2C) and in early apoptotic cells (Fig. 2D). In the latter the epichromatin remains green, however, partly locally destroyed and penetrated by inner heterochromatin domains, which become redder. Only thermal DNA denaturation at 94°C, in the presence of PFA (preventing renaturation), was able to cause the AO shift to red fluorescence of the green nuclear rim of all cells (Fig. 2E). Denaturation at 80°C gave heterogeneous epichromatin fluorescence patterns for this layer within interphase cells, while inner domains became invariably denatured (not shown). In the control for DNA denaturation, treating with

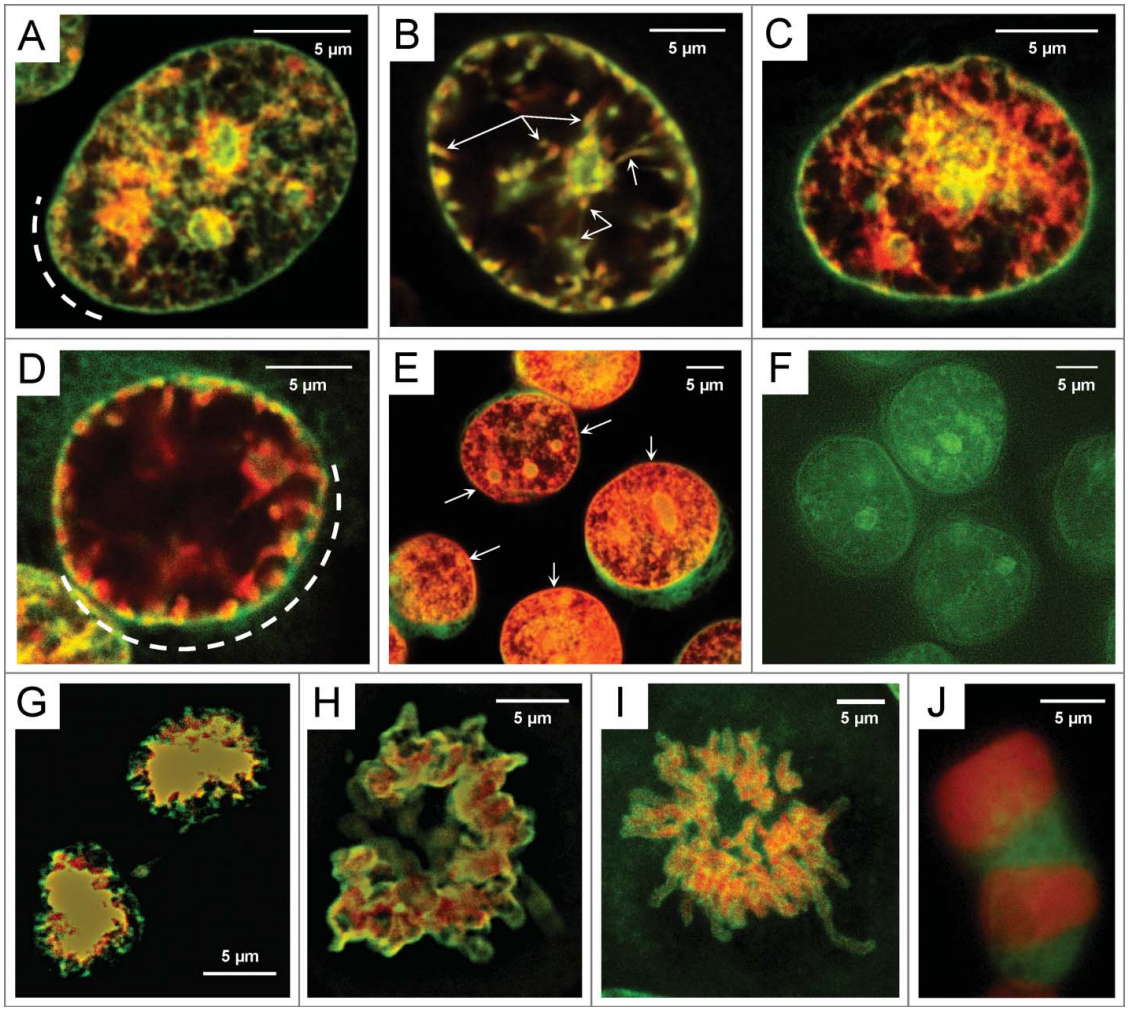

Figure 2. Testing DNA conformation with AO by confocal and epifluorescence microscopy: (A, B). Typical confocal sections of cell nuclei after conventional AO test (40 sec of HCl pre-treatment) reveal in (A) interphase and (B) early prophase green fluorescing epichromatin and adjusted patches of inner yellow/orange „sandwiched" LADs (better discriminated at the dashed segment on (A)). The arrangement and fluorescence of the layers of the heterochromatin around nucleoli are similar; on (B) the arrows indicate links of the orange, globular domains (presumed fLADs) between the perinuclear and perinucleolar compartments; (C) the enhancement of the AO metachromasy of inner LADs and perinucleolar heterochromatin, but not of the epichromatin, after more prolonged (5 min) HCl pretreatment; (D) the early apoptotic cell after conventional AO testing showing enlarged domains of inner LADs becoming redder (perfectly discriminated at the dashed segment) but not changed the green fluorescence of the epichromatin, which is penetrated at some sites by inner LADs. The metachromatic AO fluorescence in the nucleus inferior is quenched; (E) Typical confocal image of cells in AO test (after RNAse, however omitting acid pre-treatment) applying heat denaturation at 94^{0}C in the presence of PFA showing a shift of the epichromatin AO fluorescence to the red emission (arrows) – evidence of the DNA denaturation; (F) the control to (E) with cells in the same buffer treated with PFA at room temperature showing the absence of any differential orto-meta-chromatic staining of the perinuclear and perinucleolar heterochromatin – remaining green (deconvoluted image from epifluorescence with I3 optical cube); (G) anaphase in conventional AO test showing metachromasy of the chromosomes outlined by green epichromatin, particularly enriched on telomere ends (deconvoluted confocal image); (H) metaphase in AO test on the cells, shortly air-dried before fixation, showing the preservation of the epichromatin reaction with AO; (I) preservation of differential epichromatin mitotic chromosomes staining by AO after prolonged (10 min) acid pretreatment; (J) telophase tested by heat denaturation at 94^{0}C causing denaturation of the surface (epichromatin) and inner DNA (H,J – epifluorescence, I3 Leica optical cube). Bars = 5 μm.

PFA at room temperature (preserving RNAse but omitting provocative acid pre-treatment) all chromatin showed green AO fluorescence (Fig. 2F).

These results are crucial to confirm that the green AO nuclear rim (presumed to be epichromatin) indeed contains DNA, which is, however, more resistant to denaturation than LADs.

Interestingly, in the conventional AO test the range of AO fluorescence of the chromatin domains, seen under the nuclear envelope (green/yellow/orange-

red), is similar to that seen around the nucleolus (Fig. 2A). In addition, direct links can be seen between globular orange compartments, joining the nuclear periphery, and the nucleolus in very early prophase cells (Fig. 2B).

AO tested conformation of the epichromatin in mitotic cells

In mitotic cells, the AO-green fluorescing layer surrounds mitotic chromosomes, particularly richly at the telomere ends (Fig. 2G), and, contrary to interphase, it is still stainable by AO after short air-drying of cells before fixation (Fig. 2H), acid hydrolysis prolonged to 10 min (Fig. 2C), and after thermal denaturation at 80°C (not shown), however, it is not discernible from the red chromosomes after denaturation at 94°C (Fig. 2J).

Technical notes

As indicated above, in the control for DNA denaturation, treating with PFA at room temperature (preserving RNAse but omitting acid pre-treatment) all chromatin gives green AO fluorescence (Fig. 2F). Adding acid provocation after PFA fixation did not cause fluorescence bias by AO (not shown) which was obtained after ethanol/acetone fixation. This result corresponds to the reports of early (from 40-s) and further researchers of AO differential staining of DNA that paraformaldehyde is not suitable for this purpose: dehydrating fixation containing acid like Carnoy or followed by acid provocation are needed [27]. PFA covalently links DNA to many proteins, most strongly to amino-groups of lysine-rich histones, which is perfect for most morphological chromatin studies (as reviewed [28). However, in AO test this cross-linking makes the chromatin insensitive to acid provocation of the DNA-histone electrostatic binding strength, necessary for differentiation of the DNA conformation and packaging of the compared chromatin domains. It should also be noted that a green cytoplasmic halo, which was insignificant around interphase nuclei in the conventional AO test, appeared stronger in apoptosis, after prolonged acid pre-treatment, and also after DNA thermal denaturation (Fig. 2D, E). This is possibly a disadvantage of the ethanol/acetone fixation of cells, which is perfect for the DNA conformational test but not strong enough to prevent leakage of the DNA fragments. Application of DNAse I (after RNAse extraction) up to 2 h with an extensive wash in PBS/Tween 20 results in the AO test giving empty nuclei surrounded by a weak, cytoplasmic green background. The contour of the nuclear green rim becomes pale and blurred (The underlying research materials can be accessed at Suppl. Fig. 2D). This remnant fluorescence, although seen under the epifluorescence microscope could only be imaged with the x8-fold exposure as compared with the DNAse-untreated control.

In turn, immunofluorescence staining revealed, in the same experiments (DNAse I after RNAse extraction), that the cells showed well preserved lamin B and nuclear shape but almost entirely loss of DNA stainability by DAPI (which preferentially reveals AT clusters) [28] (Suppl. Fig. 2 E). Nevertheless, the stainability with the epichromatin PL2-6 antibody was still considerable, however its specificity was entirely lost – the fluorescence was rather homogenously distributed in the cell (Suppl. Fig. 2F, G). Olins and colleagues indicated in several articles [12,13,29,30] that PL2-6 is specific to epichromatin only in intact nuclei highlighting its conformational character, as in non-natural conditions PL2-6 also has affinity to separate nucleosomes and histones, and hypotonic chromatin spilled from cell nuclei. We also found decreased PL2-6 binding to the nuclear periphery in senescent cells containing DNA damage [31]. In conclusion, the advantage of both chromatin conformation methods, AO test and PL2-6, which allowed discrimination of the epichromatin as a unique fraction *in situ*, is dependent on their high sensitivity to the intact nuclear integrity and milieu.

Discussion

AO-tested conformation of epichromatin is essentially different from LADs

We judge from our data, in particular by the striking coincidence of the topology of the AO green, fluorescent, nuclear rim and the epichromatin immunostaining in interphase and mitotic cells, that both methods characterise the conformation of the same substance – the epichromatin DNA. This epichromatin conformation thus mostly prevents AO electrostatic binding and side dimerisation on neighbour DNA phosphate residues but seems favouring intercalation between base pairs. On the contrary, inner

perinuclear chromatin domains (presumably LADs) easily bind AO by side mechanism (fLADs more than cLADs) and this ability is readily enhanced by apoptosis and more prolonged acid treatment. While LADs can be thermally denatured at 80°C, the epichromatin needs 94°C for its unequivocal DNA melting in all interphase cells, as evidenced by the shift of the perinuclear rim from green to red fluorescence.

For further discussion of our results it is important to refer to the latest data obtained by Olins et al. [13] and Teif et al. [17]. In particular, these authors isolated epichromatin using chromatin immunoprecipitation by specific monoclonal PL2-6 antibody [9] followed by DNA sequencing from HL-60/S4 cells, untreated and chemically differentiated. It was found that 6541 ~ 1Kb long epichromatin domains dashed through all chromosomes were composed of the general histone octamer, however, with increased nucleosome density (also quite evident from TEM – see Fig. 1). In comparison with the general chromatin, the epichromatin domains were enriched with GC stretches but poorer for AT repeats. On the contrary, LADs are known as being enriched in long AT stretches (cLADs contain more AT repeats than fLADS) [32]. The difference in the type and proportion of prevailing reiterated sequences in three domains of the peripheral chromatin should impact DNA melting temperatures, lower for the chromatin enriched with AT (should melt at 80°C) and higher for the chromatin enriched in GC (needs 90–94°C for melting) [33]. From these considerations the following order of DNA resistance to denaturation should be expected: epichromatin>>cLADs>-fLADs. Indeed, this order was found by the degree of resistance to prolonged acid treatment, apoptotic degradation, and thermal denaturation at 80°C versus 94°C in the AO staining. The same should be subsequently the order of the strength of DNA-histone binding (nucleosome packaging density) as supporting the AO intercalation capacity [5,21,25]. Indeed, this expected order corresponds to our findings in using differentiation by short provocative acid pretreatment (40s) in the AO test for DNA conformation revealing: epichromatin/cLADs/fLADs = green/yellow/orange-red fluorescence. The caution, however, arises on possible retention of fragmented DNA by nuclear lamin, after acid provocation in the AO test, mimicking the epichromatin. However, considerable loss of its stainability by AO after DNAse treatment argues against these cautions. The origin of the remnant, weak green background needs more studies.

Moreover, and most importantly, the enrichment of epichromatin with GC stretches and highly methylated CpGs should enable the formation of the A form of the DNA double helix or B-A intermediate transition forms [34,35] favoured by the vicinity of the nuclear envelope. The reversible transition of the DNA B-form into DNA A-form double spiral occurring under dehydrating conditions and assuming a high degree of crystallinity was discovered using X-ray analysis by Rosalind Franklin and her student [36]. Currently DNA A-form is known to play an important role in prokaryote biology, response to dessication [37], some anticancer [38] and antiviral drugs [39].

The ability to bind cationic dimethyl-amino residues of the aromatic stain toluidine blue by two neighbour phosphate residues of the DNA backbone in the A-form helix was found improbable due to its too narrow minor groove [40]. However, Dearing et al [41] found that acridines prefer a mixed intercalation mechanism using both minor and major grooves, while the analysis by Sinha et al [39]. showed that the acridine derivative ethidium bromide is able to intercalate in the A-form. In one of the latest comprehensive review Mukherjee and Sasikala [19] conclude that intercalation of small, flat dyes like (acridine) proflavine is complex and exhibits several competitive intercalating pathways. Moreover, we can suggest that epichromatin may experience multiple B-A intermediate conformations [35] and possibly include the so called “DNA breathing” mechanism [42], all still far from clarity. In conclusion, the mechanism of AO monomeric binding to epichromatin DNA can allow intercalation but its details remain open for further research.

However, here it is quite sufficient to state that the epichromatin and LADS reveal by AO test the difference in their DNA-helical conformation, because this difference disappears with DNA denaturation. Moreover, this denaturation should be deep enough to melt not only AT- but also the GC-stretches enriching epichromatin. Summary of our findings and comparative literature on the difference between epichromatin and inner peripheral chromatin domains (LADs) is presented in Table 1.

Table 1. The distinctive features of the epichromatin and LADs.

Features	Epichromatin 5% DNA	LADs 40% DNA
Primary DNA structure enriched	GC stretches [17]	AT stretches [32]
Domain size	~ 1Kbp	0.1–10 Mbp
Nucleosome repeat	Octamer	Octamer
Nucleosome occupancy	Dense [17]	Less dense[a]
Supranucleosome packaging (glutaraldehyde fixation)	30–35 nm superbeads[b]	30 nm fibers
AO fluorescence in DNA structural test	Green (monomere binding prevails)	Orange-red (dimere binding prevails)
DNA denaturability	94°C	80°C
DNAse	Resistant[c]	Sensitive
Hydrophobicity	Yes	No
Histone H3 epigenetic marks	Not at all?[d]	Mostly repressive [2,4]

[a] seen on Fig.1; [b]deduced in this paper, see the paragraph in Discussion on that; [c]after cross-linking to nuclear envelope as performed by[7]. [d]In the immunoprecipitation study[17], six tested epigenetic histone H3 markers, activating and repressive, did not bind epichromatin, both in untreated and differentiated HL-60/S4 cells.

Next we should like to discuss the supranucleosomal packaging of the epichromatin.

The epichromatin is most likely packed in supranucleosomal superbeads and organized by hydrophobic interactions

The average length of epichromatin domains revealed by ChIP-seq is ~1Kb [13]. This size coresponds to one pitch (~ 6 nucleosomes) of the 30 nm supranucleosomal zigzag ribbon model. This type of supranucleosome folding is based on the di-nucleosome periodicity, established as the first step in the organization of the higher order chromatin structure [43–45]. Solenoid, zig-zag, and superbead models are considered as topologically equivalent patterns of the chromatin packaging revealed after aldehyde fixations [5,46–48], however, in situ all three patterns, as well as 10-nm 'beads-on a string" are often observed in a mix, very sensitive to intranuclear mileu [5,49,50]. Currently even less ordered chromatin structure is also considered as a “melt” model based on freeze-EM results [51]. However investigations of the ELCS including epichromatin still revealed that proximity to the nuclear membrane imposes order on the in vivo 10-nm chromatin fibers and favours in ELCS under chemical fixation the regular rod-like pattern, based on di-nucleosome periodicity [52]. In line with these results, the detailed recent analysis has shown that di-nucleosome periodicity is mostly characteristic for the DNAse low-sensitive chromatin enriched with GC-dinucleotides, while AT-rich regions are more readily digested up to mononucleosomes [53]. It follows that zig-zag ribbon model based on di-nucleosomic periodicity is well applicable for the DNAse-resistant epichromatin which is enriched with GC stretches. We suggest therefore that a pitch of the supranucleosomal zig-zag ribbon corresponds to one ~1Kb domain of epichromatin determined by ChIP-seq analysis. Moreover, GC-enrichment favours assuming by its DNA of hydrophobic A-form or intermediate conformations further packaged in nucleosome superbeads, thus minimizing its surface in the lipid microenvironment of the nuclear envelope (schematics on Fig 3, A and B). The short domains of epichromatin are dashed between long segments of AT-enriched LAD parts and along the whole length of chromosomal DNA thread [9,13]. We further speculate that epichromatin domains, packed in dense superbeads, stack together in a nanoparticle-like monolayer at the inner nuclear membrane by hydrophobic interactions being excluded from the nuclear interior by water and repulsed by the hydrated garlands of intermitting AT-repeat-rich long LADS domains (Fig. 3C). It therefore follows that the integrity and ternary/quaternary structure of the epichromatin layer is dependent not only on its own chemical binding to amphipathic proteins and phosphatidylserine of the inner nuclear envelope [9,11,30] but also physically (by self-assembly) on the lipid micro-environment of the nuclear envelope and possibly also the integrity of the counteracting LADs. If not cross-linked to nuclear envelope proteins (e.g., by chemically neutral UV as performed in [7]) the relatively DNAse-resistant epichromatin can lose organisation by treatment with DNAse as we have seen in our experiments. The fLADs with a relatively small content of AT-rich satellite DNA and better hydrated than cLADs, are located further inside the cell nucleus and represent the most mobile heterochromatin fraction between two determinants of the cell nucleus organisation – the nuclear envelope and the nucleolus. It is clear that active euchromatin (not depicted on our scheme) can loop even further inside the cell nucleus [1] or is accessible at nuclear pores. Our observations on the similar pattern of AO layered gamut in the perinuclear and perinucleolar heterochromatin are in accord with the considerable

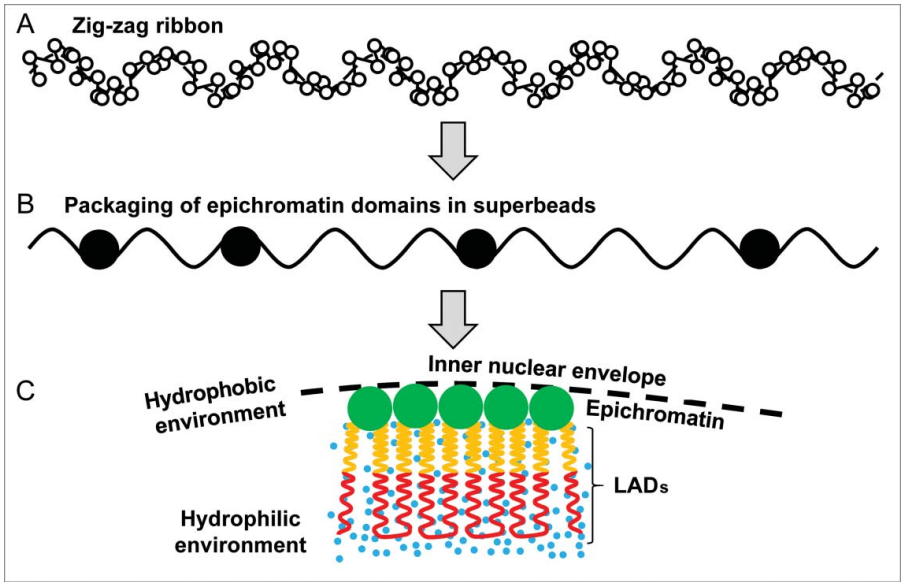

Figure 3. Hypothetical schematics of the supranucleosomal packaging and orientation of the epichromatin and inner LADs in cell nucleus: (A) zig-zag ribbon of the di-nucleosomal units including ~ 6 nucleosome per zig-zag pitch (reproduced from [5, citing Yamamoto et al [48]); (B) – packaging of ~ 1Kbp epichromatin domains corresponding to one pitch of the zig-zag ribbon into superbeads alternating with less densely packed ribbon segments of the inner LADs; (C) the intranuclear arrangement of epichromatin superbeads under the nuclear envelope stacked by hydrophobic forces and repulsed from alternating, inner LADs, whose garlands are situated in the hydrophilic nuclear interior. The colours correspond to the range of AO staining in the DNA structural test. For simplicity the relative size of the chromatin superbeads on (C) is disproportionately enlarged.

overlay of heterochromatic LADs and nucleolar associated domains (NADs) found by Hi-C capture and DamID tagging techniques, suggesting the transit between LADs and NADs and also showing the involvement of mobile fLADs in transcription [2,4,54–56].

The relative hydrophobicity of epichromatin also explains its location at the surface of the mitotic chromosomes, enabling the attraction of the amphipathic lamin B receptor and LAP2β, later also lamin B with the ER vesicles of the reconstituting nuclear envelope to decondensing chromosomes in mitotic telophase, thus re-establishing the nuclear order. Our findings support and complement the "epichromatin hypothesis" by Olins and colleagues [9], suggesting that this evolutionary conserved chromatin may play a crucial role in organizing interphase nucleus architecture.

Materials and methods

Cell culture

MCF-7 human breast cancer cell line (ATCC) was cultured in Dulbecco's modified Eagle's media (DMEM) supplemented with 10% fetal bovine serum (FBS, Sigma). Cells were grown on chamber-slides without antibiotics in 5% CO_2 in an incubator at 37°C.

Acridine orange (AO) DNA structural test

Cells in chamber slides were washed with warm PBS, covered with FBS (excess then removed) and immediately fixed in ethanol/acetone (1:1) for 1h at 4°C. After fixation the slides were passed through decreasing grades of ethanol (96%, 90%, 70%) to PBS. The slides were then treated with RNAse A (DNAse and protease free, 10 mg/ml, Thermo scientific #EN0531) in PBS for 30 min at 37°C and then rinsed in PBS. Afterwards hydrolysis for 40 sec at 60°C in 1N HCl was performed. In some experiments hydrolysis was prolonged to 5–10 min. After hydrolysis the slides were washed in three changes of distilled water (1 min each), passed through PBS for 2 min and 0.1 M acetic buffer pH 4.1 for 5min. Staining with high purity AO (Polyscience Inc) in concentration 10^{-4} M was performed in the same buffer for 15 min (in the dark) followed by three 5 min changes of AO diluted to concentration 10^{-6} M in the same acetic buffer and immediately sealed in the latter solution under a glass coverslip with nail polish.

For DNA thermal denaturation experiments after RNAse treatment the slides were incubated in the presence of freshly prepared 4% paraformaldehyde (PFA) in SSC (pH 7) for 20min at 80°C or 94°C followed by incubation in ice cold SSC for 5min. PFA was added during the denaturation step as advocated by Rigler [18,26] to prevent DNA renaturation. In this case HCl treatment was omitted and slides were directly passed to the AO staining steps. As a control for DNA denaturation incubation in 4% PFA at room temperature was performed.

In some experiments, after RNAse treatment, application of DNAse I (Sigma, D-4263) 200U/ml (in reaction buffer for DNAse I (Fermentas) containing 5mM $MgCl_2$) for DNA extraction was performed for 40 min or 2 h at 37°C. After DNAse treatment extensive washing in PBS/ 0.1% Tween 20 twice for 10 min was carried out.

Immunofluorescence

For immunofluorescent staining of lamin B1 and epichromatin we started with the basic protocol of the AO structural test (including fixation in ethanol/acetone and RNAse pre-treatment). After RNAse or RNAse and DNAse treatments the additional fixation in 4% PFA for 15 min at RT was also carried out. The slides were then washed thrice in PBS 0.1 M glycine for 5 min, once for 5min in PBS and once in TBS 0.01% Tween 20 (TBST) for 5 min. They were subsequently blocked for 15 min in TBS, 0.05% Tween 20, 1% BSA at room temperature. Samples were covered with TBS, 0.025% Tween 20, 1% BSA containing primary antibodies for lamin B1 (Abcam, ab1604, rabbit polyclonal) and mouse monoclonal PL2-6 for epichromatin (kind donation of Donald Olins) and incubated overnight at 4°C in a humid chamber. Samples were then washed thrice in TBST and covered with TBST containing the appropriate secondary antibodies (Goat anti-mouse IgG Alexa Fluor 488 (A31619, Invitrogen) and Goat anti-Rabbit-IgG Alexa Fluor 594 (A31631, Invitrogen) and incubated for 40 min at room temperature in the dark. Slides were washed thrice for 5 min with TBST and once for 2 min in PBS. Samples were then counterstained with 0.25 μg/ml DAPI for 2 min, and finally embedded in Prolong Gold (Invitrogen).

Microscopy and AO spectrum analysis

AO stained slides were analysed and images acquired using an epifluorescence microscope Leica DM LS2, equipped with a Sony DXC-S500 colour video camera, and using a Leica 100x ∞/0.17 C Plan NA = 1,25 oil immersion objective. The fluorescence filter cube Leica I3 was used (excitation filter BP 420–490 nm, dichromatic mirror 510 nm, suppression filter LP 515 nm). Images were also acquired using confocal laser scanning microscope Leica DM RA-2, equipped with a TCS-SL confocal scanning head. Two objectives were used: N Plan 100x NA = 1.25 Oil RC objective and 63x NA = 1.4 oil immersion objective. AO was excited with an Argon-ion laser (excitation 488 nm) and emission was detected between 520 and 540 nm to obtain AO monomers fluorescence and between 630 and 660 nm to obtain AO polymers fluorescence. The acquired images were analysed using Image-Pro Plus 4.2 (Media Cybernetics) and ImageJ 1.51 h (National Institutes of Health).

The AO fluorescence spectrum was detected using Nikon A1+ confocal laser scanning microscope, equipped with Plan Apo 100x NA = 1.4 Oil Ph3 objective and was excited with 488 nm (Argon-ion laser). The emission spectrum was detected between 515 and 655 nm with a step 10 nm.

Disclosure of potential conflicts of interest

No potential conflicts of interest were disclosed.

Acknowledgments

Ada and Donald Olins are acknowledged for kind donation the PL2-6 antibody for epichromatin. We are grateful to Mr. Roger Alston for English editing of the manuscript. The support of EuroCellNet COST Action CA15214 is acknowledged.

Funding

Latvijas Zinātnes Padome; Latvijas Universitāte [2012/341].

ORCID

Jekaterina Erenpreisa http://orcid.org/0000-0002-2870-7775

References

[1] Guelen L, Pagie L, Brasset E, et al. Domain organization of human chromosomes revealed by mapping of nuclear lamina interactions. Nature. 2008;453(7197):948–951. doi:10.1038/nature06947.

[2] Kind J, Pagie L, Ortabozkoyun H, et al. Single-Cell Dynamics of Genome-Nuclear Lamina Interactions. Cell. 2013;153(1):178–192. doi:10.1016/j.cell.2013.02.028.

[3] Amendola M, van Steensel B. Mechanisms and dynamics of nuclear lamina–genome interactions. Curr Opin Cell Biol. 2014;28:61–68. doi:10.1016/j.ceb.2014.03.003.
[4] Pombo A, Dillon N. Three-dimensional genome architecture: players and mechanisms. Nat Rev Mol Cell Biol. 2015;16(4):245–257. doi:10.1038/nrm3965.
[5] Erenpreisa J.. *Chromatin Organization in Interphase Cell Nucleus*. Riga: Zinatne Publ; 1990.
[6] Davies HG. Electron-microscope observations on the organization of heterochromatin in certain cells. J Cell Sci. 1968;3(1):129–150.
[7] Fais D, Prusov AN, Polyakov VYu. The anchorosome, a special chromatin granule for the anchorage of the interphase chromosome to the nuclear envelope. Cell Biol Int Rep. 1989;13(9):747–758. doi:10.1016/0309-1651(89)90052-0.
[8] Olins DE, Olins AL. Nuclear envelope-limited chromatin sheets (ELCS) and heterochromatin higher order structure. Chromosoma. 2009;118(5):537–548. doi:10.1007/s00412-009-0219-3.
[9] Olins AL, Langhans M, Monestier M, et al. An epichromatin epitope: persistence in the cell cycle and conservation in evolution. Nucleus. 2011;2(1):47–60. doi:10.4161/nucl.13655.
[10] Losman MJ, Fasy TM, Novick KE, et al. Monoclonal autoantibodies to subnucleosomes from a MRL/Mp(-)+/+ mouse. Oligoclonality of the antibody response and recognition of a determinant composed of histones H2A, H2B, and DNA. J Immunol. 1992;148(5):1561–1569. http://www.ncbi.nlm.nih.gov/pubmed/1371530. Accessed November 19, 2017.
[11] Prudovsky I, Vary CPH, Markaki Y, et al. Phosphatidylserine colocalizes with epichromatin in interphase nuclei and mitotic chromosomes. Nucleus. 2012;3(2):200–210. doi:10.4161/nucl.19662.
[12] Olins AL, Rhodes G, Welch DBM, et al. Lamin B receptor: multi-tasking at the nuclear envelope. Nucleus. 2010;1(1):53–70. doi:10.4161/nucl.1.1.10515.
[13] Olins AL, Ishaque N, Chotewutmontri S, et al. Retrotransposon Alu is enriched in the epichromatin of HL-60 cells. Nucleus. 2014;5(3):237–246. doi:10.4161/nucl.29141.
[14] Haynes ME, Davies HG. Observations on the Origin and Significance of the Nuclear Envelope-Limited Monolayers of Chromatin Unit Threads associated with the Cell Nucleus. J Cell Sci. 1973;13(1):139–171.
[15] Olins AL, Buendia B, Herrmann H, et al. Retinoic Acid Induction of Nuclear Envelope-Limited Chromatin Sheets in HL-60. Exp Cell Res. 1998;245:91–104. doi:10.1006/excr.1998.4210.
[16] Erenpreisa J, Ivanov A, Cragg M, et al. Nuclear envelope-limited chromatin sheets are part of mitotic death. Histochem Cell Biol. 2002;117(3):243–255. doi:10.1007/s00418-002-0382-6.
[17] Teif VB, Mallm J-P, Sharma T, et al. Nucleosome repositioning during differentiation of a human myeloid leukemia cell line. Nucleus. 2017;8(2):188–204. doi:10.1080/19491034.2017.1295201.
[18] Rigler R. Chapter 3: The Binding of Acridine Orange to Nucleic Acids Influence of the nucleic acids' secondary structure. Acta Physiol Scand. 1966;67(s267):32–51. doi:10.1111/j.1748-1716.1966.tb03357.x.
[19] Mukherjee A, Sasikala WD. Drug–DNA Intercalation. In: Advances in Protein Chemistry and Structural Biology. 2013;Vol 92:1–62. doi:10.1016/B978-0-12-411636-8.00001-8.
[20] Erenpreiss J, Bars J, Lipatnikova V, et al. Comparative study of cytochemical tests for sperm chromatin integrity. J Androl. 2001;22(1):45–53.
[21] Amado AM, Pazin WM, Ito AS, et al. Acridine orange interaction with DNA: Effect of ionic strength. Biochim Biophys Acta – Gen Subj. 2017;1861(4):900–909. doi:10.1016/j.bbagen.2017.01.023.
[22] Evenson D, Darzynkiewicz Z, Jost L, et al. Changes in accessibility of DNA to various fluorochromes during spermatogenesis. Cytometry. 1986;7(1):45–53. doi:10.1002/cyto.990070107.
[23] Darzynkiewicz Z. Acid-induced denaturation of DNA in situ as a probe of chromatin structure. Methods Cell Biol. 1994;41:527–541. doi:10.1016/S0091-679X(08)61738-0.
[24] Erenpreisa J, Freivalds T, Roach H, et al. Apoptotic cell nuclei favour aggregation and fluorescence quenching of DNA dyes. Histochem Cell Biol. 1997;108(1):67–75. doi:10.1007/s004180050147.
[25] Erenpreiss J, Spano M, Erenpreisa J, et al. Sperm chromatin structure and male fertility: biological and clinical aspects. Asian J Androl. 2006;8(1):11–29. doi:10.1111/j.1745-7262.2006.00112.x.
[26] Roschlau G. Ein Betrag zum histochemischen Verhalten der Kern DNS in Interphase und Mitoze dargestellt durch kombinierte Saurenhydro- lyse und Akridinorange fluoro-chromierung. Histochemistry. 1965;5:396–406. doi:10.1007/BF00306291.
[27] Rigler R. Microfluorometric characterization of intracellular nucleic acids and nucleoproteins by acridine orange. Acta Physiol Scand Suppl. 1966;267:1–122.
[28] Chazotte B. Labeling nuclear DNA using DAPI. Cold Spring Harb Protoc. 2011;2011(1):pdb.prot5556. doi:10.1101/pdb.prot5556.
[29] Olins A, Zwerger M, Herrmann H, et al. The human granulocyte nucleus: Unusual nuclear envelope and heterochromatin composition. Eur J Cell Biol. 2008;87(5):279–290. doi:10.1016/j.ejcb.2008.02.007.
[30] Gould TJ, Tóth K, Mücke N, et al. Defining the epichromatin epitope. Nucleus. 2017;8(6):625–640. doi:10.1080/19491034.2017.1380141.
[31] Huna A, Salmina K, Erenpreisa J, et al. Role of stress-activated OCT4A in the cell fate decisions of embryonal carcinoma cells treated with etoposide. Cell Cycle. 2015;14(18):2969–2984. doi:10.1080/15384101.2015.1056948.
[32] Meuleman W, Peric-Hupkes D, Kind J, et al. Constitutive nuclear lamina-genome interactions are highly conserved and associated with A/T-rich sequence. Genome Res. 2013;23(2):270–280. doi:10.1101/gr.141028.112.

[33] Yakovchuk P, Protozanova E, Frank-Kamenetskii MD. Base-stacking and base-pairing contributions into thermal stability of the DNA double helix. Nucleic Acids Res. 2006;34(2):564–574. doi:10.1093/nar/gkj454.

[34] Ng H-L, Dickerson RE. Mediation of the A/B-DNA helix transition by G-tracts in the crystal structure of duplex CATGGGCCCATG. Nucleic Acids Res. 2002;30 (18):4061–4067. doi:10.1093/nar/gkf515.

[35] Vargason JM, Henderson K, Ho PS. A crystallographic map of the transition from B-DNA to A-DNA. Proc Natl Acad Sci U S A. 2001;98(13):7265–7270. doi:10.1073/pnas.121176898.

[36] Franklin RE, Gosling RG. Molecular configuration in sodium thymonucleate. Nature. 1953;171(4356):740–741. doi:10.1038/171740a0.

[37] Whelan DR, Hiscox TJ, Rood JI, et al. Detection of an en masse and reversible B- to A-DNA conformational transition in prokaryotes in response to desiccation. J R Soc Interface. 2014;11(97):20140454–20140454. doi:10.1098/rsif.2014.0454.

[38] Gelasco A, Lippard SJ. Anticancer Activity of Cisplatin and Related Complexes. In: *Metallopharmaceuticals I*. Berlin, Heidelberg: Springer Berlin Heidelberg; 1999.p. 1–43. doi:10.1007/978-3-662-03815-4_1.

[39] Sinha R, Islam MM, Bhadra K, et al. The binding of DNA intercalating and non-intercalating compounds to A-form and protonated form of poly(rC)·poly(rG): Spectroscopic and viscometric study. *Bioorg Med Chem*. 2006;14 (3):800–814. doi:10.1016/j.bmc.2005.09.007.

[40] Sato S, Matsumoto S, Freivalds T, et al. Consideration on the Metachromatic Spectra of Toluidine Blue Dimers Formed on DNA Oligomers. Bull Chem Soc Jpn. 2010;83 (10):1216–1222. doi:10.1246/bcsj.20100032.

[41] Dearing A, Weiner P, Kollman PA. Molecular mechanical studies of proflavine and acridine orange intercalation. Nucleic Acid Res. 1981;9(6):1483–97. doi:10.1093/nar/9.6.1483.

[42] Sobell HM. Premeltons in DNA. J Struct Func Genomics. 2016;17(1):17–31. doi:10.1007/s10969-016-9202-4.

[43] Pospelov, Svetlikova 1982 Higher order chromatin structure determines double-nucleosome periodicity of DNA fragmentation. Mol Biol Rep. 1982;8(2):117–22. doi:10.1007/BF00778514.

[44] Kato M, Onishi Y, Wada-Kiyama Y, et al. Dinucleosome DNA of human K562 cells: experimental and computational characterizations. J Mol Biol. 2003;332 (1):111–125. doi:10.1016/S0022-2836(03)00838-6.

[45] Kato D, Osakabe A, Arimura Y, et al. Crystal structure of the overlapping dinucleosome composed of hexasome and octasome. Sci. 2017;356(6334):205–208. doi:10.1126/science.aak9867.

[46] Alberts B, Johnson A, Lewis J, et al. DNA, Chromosomes, and Genomes. In: *Molecular Biology of the Cell*. 6th ed. New York: Garland Science; 2015.p. 173–236.

[47] Subirana JA, Muñoz-Guerra S, Aymamí J, et al. The layered organization of nucleosomes in 30 nm chromatin fibers. Chromosoma. 1985;91(5):377–390. doi:10.1007/BF00291012.

[48] Yamamoto. Supranucleosomal packing in 30 nm chromatin fibers. In: *.Proc. 11th Int Congress Electron Microscopy*. Kyoto; 1986;2447–2448.

[49] Wu C, Bassett A, Travers A. A variable topology for the 30-nm chromatin fibre. EMBO Rep. 2007;8(12):1129–1134. doi:10.1038/sj.embor.7401115.

[50] Erenpreisa J, Zaleskaya N. Effect of triton X-100 on cytochemical and ultrastructural pattern of chromatin. Acta Morphol Hung. 1983;31(4):387–393.

[51] Fudenberg G, Mirny LA. Higher order chromatin structure: bridging physics and biology. Curr Opin Genet Dev. 2012;22(2):115–24. doi:10.1016/j.gde.2012.01.006.

[52] Eltsov M, Sosnovksi S, Olins A, et al. ELCS In Ice: Cryoelectron Microscopy Of Nuclear Envelope Limited Chromatin Sheets. Pharm Sci Fac Posters. 2014;123:303–12.

[53] Chereji R V., Kan T-W, Grudniewska MK, et al. Genome-wide profiling of nucleosome sensitivity and chromatin accessibility in Drosophila melanogaster. Nucleic Acids Res. 2016;44(3):1036–1051. doi:10.1093/nar/gkv978.

[54] van Koningsbruggen S, Gierlinski M, Schofield P, et al. High-resolution whole-genome sequencing reveals that specific chromatin domains from most human chromosomes associate with nucleoli. *Mol Biol Cell*. 2010;21 (21):3735–3748. doi:10.1091/mbc.E10-06-0508.

[55] Németh A, Conesa A, Santoyo-Lopez J, et al. Initial Genomics of the Human Nucleolus. Akhtar A, ed. PLoS Genet. 2010;6(3):e1000889. doi:10.1371/journal.pgen.1000889.

[56] Padeken J, Heun P. Nucleolus and nuclear periphery: Velcro for heterochromatin. Curr Opin Cell Biol. 2014;28:54–60. doi:10.1016/j.ceb.2014.03.001.